34th Annual International Conference of the IEEE EMBS
San Diego, California USA, 28 August - 1 September, 2012

Melanoma screening system using hyperspectral imager attached to imaging fiberscope*

T. Nagaoka, *Member*, *IEEE*, A. Nakamura, Y. Kiyohara and T. Sota, *non-Member, IEEE*

Abstract— **Early detection and proper excision of the primary lesions of melanoma are crucial for reducing melanoma-related deaths. In order to support the early detection of melanoma, melanoma screening systems have been extensively studied and developed. Recently we have proposed a melanoma discrimination index derived from hyperspectral data (HSD) in the visible-near infrared wavelength region. The index represents variegation in spectra over a lesion and works well in discriminating melanoma from other pigmented lesions. However the previous hyperspectral imager did not have an enough allowance for measurement of lesions. To overcome the problem with it, we have developed a hyperspectral imager attached to imaging fiberscope. This equipment has been able to accumulate HSD in a view field of ϕ40 mm within about 10 seconds, from which the above-mentioned melanoma discrimination index has been calculated. Performance of the system has been studied in nine cases of melanoma and 18 cases of non-melanoma, obtained from patients and volunteers, all of whom were Japanese. The index has achieved a sensitivity of 100 % and a specificity of 94.4 %.**

I. Introduction

In Japan, the number of death from melanoma is increased to 1.7 times [1], the number of patient is increased to 5.0 times [2, 3] from 1975 to 2005. Prognosis of melanoma strongly depends on its early stage detection and subsequent excision. However, the diagnosis accuracy of melanoma by naked eyes has been reported to be about 56% even by a specialist in dermatology [4]. The ABCD rule has considerably improved the early detection of melanoma [5]. Dermoscopy has opened a door to diagnose pigmented skin lesions (PSLs) from the view point of morphology [6-11]. It is well known that dermoscopy improves accuracy in diagnosing PSLs [12, 13]. Nevertheless, diagnosis based on the ABCD rule with dermoscopy is still subjective and associated with low reproducibility.

In order to overcome the subjectivity of dermoscopy, a great number of researchers have challenged to develop computer-aided-automatic melanoma screening systems [14-18]. They use color dermoscopy images or multispectral images. Parameters used in differentiating melanoma from other PSLs, are derived from those digital images using various image processing techniques. However, these parameters are of quite different type from those microscopically evaluated by pathologists to determine the presence of malignancy [15].

Essence of melanoma is reflected in its morphology. Difference in morphology of PSLs is predominantly determined by difference in spatial distribution and concentration of melanin and hemoglobin molecular. These information is carried in cutaneous reflectance spectra. Focusing on this fact, we have previously reported a hyperspectral imager (HSI) as a spectroscopic melanoma screening system based on hyperspectral imaging technique [19, 20] and proposed a melanoma discrimination index derived from hyperspectral data (HSD) [21]. The index represents variegation in spectra stored in one set of HSD. That is, the higher the malignance is, the larger the index is. The index has been highly successful in discriminating melanoma from non-melanoma on non-globular skin of Japanese though the statistical population is small.

The problem with previous HSI was its size and, consequently, to force subjects to pose in unnatural position depending on PSLs' locations. Using fiber optics is one of promising candidates to overcome the problem [22,23]. Then, it is important to use imaging fiberscope in order to acquire HSD. In this article we report a melanoma screening system consisting of HSI and imaging fiberscope. The system uses the same melanoma discrimination index as previously proposed. Performance of the system is also reported. Although a statistical population is still small, it is revealed that the index is useful in differentiating melanoma from other PSLs.

II. Methods and Patients

A. Methods

A HSI attached to imaging fiberscope was developed. For details in mechanisms of HSI, see reference 21. Its core part consisted of an imaging spectrograph (ImSpector V8E, Specim, Oulu, Finland) and electron multiplying charge-coupled device (LucaS, Andor Technology, Belfast, Northern Ireland). Figure 1 shows a photograph of the system (a) and a schematic optical diagram (b). An imaging fiberscope used herein was GIF-P30 (Olympus, Japan). Its

* This work was partially supported by the City Area Program (Fuji Area Cooperation of Innovative Technology & Advanced Research in Evolution Area, Development Stage 2007-2009) of the Ministry of Education, Culture, Sports, Science, and Technology, the Prototype Validation/Practical Realization Program for Advanced Measurement and Analysis (Program-P), Japan Science and Technology Agency and KAKENHI (23700584) of the Japan Society for the Promotion of Science.

T. Nagaoka and T. Nakamura is with the Waseda Research Institute for Science and Engineering, Waseda University, Shinjuku, Tokyo 169-8555, Japan (corresponding author to provide phone: +81-(0)55-989-5222; fax: +81-(0)55-959-6085; e-mail: nagaoka@aoni.waseda.jp).

Y. Kiyohara is with the Dermatology Division, Shizuoka Cancer Center, Nagaizumi, Shizuoka 411-9777, Japan.

T. Sota is with the Department of Electrical Engineering and Bioscience, Waseda University, Shinjuku, Tokyo 169-8555, Japan.

focal distance was 15 mm and its view field was ϕ40 mm. A cylinder-shaped cover was attached to the tip of the fiberscope to keep the focal distance, to reject stray light and to prevent an excess pressure impeding the blood circulation [24], see Figure 1 (c).

The melanoma discrimination index was derived from HSD, for detail, see reference 21. A brief explanation is as follows. An averaged spectrum obtained from the upper arm of a typical healthy Japanese volunteer (case No. 24) was defined as a reference spectrum. Each spectrum stored in a HSD was compared with the reference spectrum using a spectral angle [25]. Normalized frequency distribution of spectral angle represents variegation in the spectra, which is nothing but irregularity, disorder and variation in morphology. The normalized frequency distribution of spectral angle was numerically evaluated using the entropy concept to obtain the discrimination index.

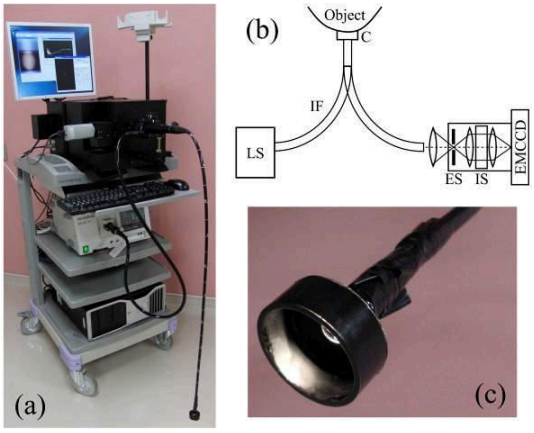

Figure 1. A hyperspectral imager for pigmented skin lesions. A photograph (a) and schematic optical diagram (b) and Skin-Fiber Interface (c). See the text for details. LS, light source with 150 W halogen lamp; IF, imaging fiverscope; C, skin-fiber interface; IS, imaging spectrograph; ES, entrance slit; EMCCD, electron multiplication CCD camera.

B. Patients

This study was approved by the Institutional Review Board of Shizuoka Cancer Center (SCC). Written informed consent was obtained before measurements were made. Twenty-seven patients who had consulted the SCC were registered for this research from July 2008 to April 2011. Features of these PSLs are summarized in TABLE I. There was no significant difference in age, sex and size of lesion between melanoma and non-melanoma groups.To evaluate the performance of our system reliably, cases who had inflammation and exudates were excluded. Pigmented lesions of the nail were excluded. All subjects were Japanese.

Nine PSLs were clinically suspected to be malignant and histopathological evaluation of biopsy specimens confirmed the diagnosis of melanoma. These PSLs were 2 acral lentiginous melanoma (ALM), 4 lentigo maligna melanoma (LMM), 2 superficial spreading melanoma (SSM) and 1 nodular melanoma (NM). The remaining 18 PSLs were 1 basal cell carcinoma (BCC), 12 seborrheic keratosis (SK) and 5 nevus.

C. Statistical evaluation

Statistically significant differences between the melanoma and non-melanoma groups were analyzed using the Mann-Whitney U-test. A p-value less than 0.05 was considered statistically significant. Because the number of samples was small, the jackknife method was used to minimize bias, instead of cross-validation. In this approach, one sample is excluded from all samples and discriminant analysis is performed, and the excluded sample is discriminated with the use of the discriminant coefficient so obtained. The same procedure was executed for all samples, and sensitivity and the specificity were calculated from the results of the discriminant analysis. Receiver operating characteristic (ROC) analysis on reference 26 was also performed for purposes of future study.

TABLE I. LESIONS ANALYZED IN THE PRESENT STUDY.

Case No.	Sex/Age	Diagnosis	Size of Lesion, mm	Site of Lesion	Index
1	M/71	ALM	37 x 24	extremities	4.84
2	M/80	ALM	> 50	extremities	4.97
3	F/80	LMM	12 x 8	head and neck	5.01
4	F/70	LMM	> 20	head and neck	4.71
5	F/83	LMM	40 x 30	head and neck	4.64
6	M/52	LMM	30 x 25	trunk	5.11
7	M/62	SSM	14 x 12	trunk	5.68
8	M/47	SSM	17 x 11	extremities	4.72
9	F/44	NM	9 x 7	extremities	4.63
10	M/56	BCC	20 x 20	head and neck	4.41
11	M/65	SK	8 x 7	head and neck	4.09
12	M/58	SK	10 x 9	head and neck	4.15
13	M/55	SK	14 x 14	head and neck	3.94
14	M/47	SK	30 x 30	head and neck	4.12
15	F/72	SK	13 x 8	trunk	3.25
16	M/70	SK	12 x 8	trunk	4.52
17	M/58	SK	11 x 9	trunk	4.19
18	F/83	SK	14 x 11	trunk	4.06
19	M/74	SK	27 x 20	extremities	3.80
20	F/65	SK	8 x 8	extremities	4.38
21	F/86	SK	16 x 12	extremities	4.84
22	M/64	SK	10 x 9	extremities	4.38
23	M/33	Nevus	3 x 3	extremities	3.96
24	M/31	Nevus	13 x 10	extremities	3.74
25	F/35	Nevus	13 x 5	extremities	3.56
26	M/52	Nevus	3 x 3	extremities	3.56
27	M/23	Nevus	5 x 5	extremities	3.60

ALM: Acral Lentiginous Melanoma
LMM: Lentigo Maligna Melanoma
SSM: Superficial Spreading Melanoma
NM: Nodular Melanoma
SK: Seborrheic Keratosis
Nevus: Nevus Cell Nevus

III. RESULTS

Two-dimensional spectral angle-color maps are shown in Figure 2 for typical cases of (a) a SSM (case No.7), (b) a SK (case No. 15) and (c) a melanocytic nevus (case No. 23). The corresponding indices have been calculated to be 4.72, 4.09 and 3.74, respectively. Figure 3 reveals that the spectral angles are more widely distributed for melanoma (case No. 7) than for non-melanoma (case No. 23). The index is thus larger for melanoma than for non-melanoma. It should be noted that variegation in spectra doubles when the index increases by unity. This is because a binary logarithmic function is included in the calculation of the index.

Box-and-whisker plots of indices for the two groups are shown in Figure 4 (a). The Mann-Whitney U-test revealed that the difference in the two groups is statistically significant.

Figure 4 (b) shows the ROC curve. The area under the curve, AUC, was 0.97, revealing that the index is useful for distinguishing melanoma from non-melanoma. As a result of the discriminant analysis, the optimum threshold value was determined to be 4.56. A sensitivity of 100% and a specificity of 94.4% were obtained by applying this threshold value to the present data set.

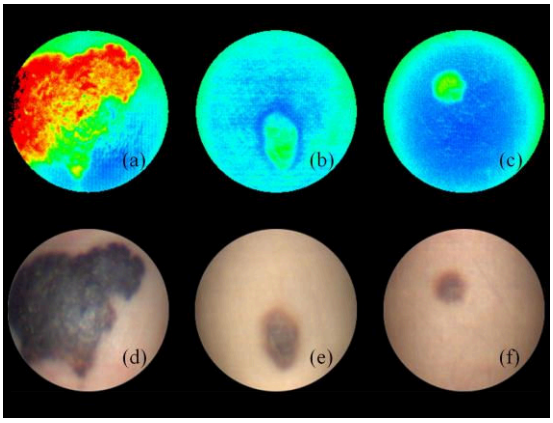

Figure 2. False-color, two-dimensional angle map (a), (b), (c) and the corresponding false color images (d), (e), (f) for a peripheral part of sperficial spreading melanoma of case No. 7, a peripheral part of seborrheic keratosis of case No. 15 and a melanocytic nevus of case No. 23. In the seborrheic keratosis and a melanocytic nevus, the boundary of the lesion is characterized by a melanin-dominant region, and can be clearly distinguished from normal skin, which is a hemoglobin-dominant region. In contrast, the invasive nature of the melanoma is reflected by nesting of the melanin-dominant region within the hemoglobin-dominant region.

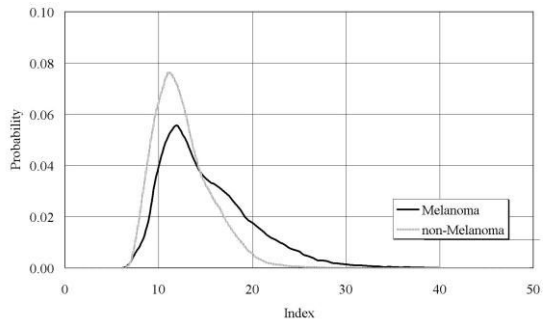

Figure 3. Normalized frequency distribution of spectral angle for melanoma of case No. 7 (black curve) and non-melanoma of case No. 23 (gray curve). The overall features of the probability curve for the non-melanoma are obviously different from those for the melanoma. Differences in such overall features of the curve produce the difference in the index.

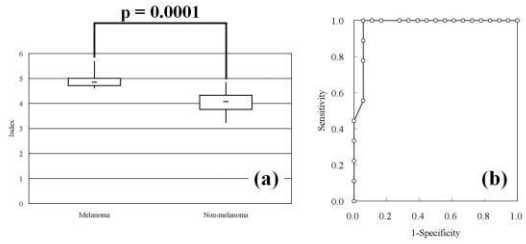

Figure 4. Box and whisker plots of indices for the melanoma (left hand side) and non-melanoma group (right hand side) (a) and ROC curve (b). AUC reaches to 0.97. These results show that the index is useful in discriminating melanoma from non-melanoma.

IV. Discussion

It is well known that dermoscopy has introduced a new morphologic dimension in the diagnosis of melanoma. The ABCD rule of dermoscopy [27] summarizes guidelines for diagnosis based on expression of malignancy or the invasive nature of a melanoma at the morphologic level. The morphology of PSLs is dominantly determined by spatial change in the concentration of melanin and hemoglobin molecular. The index used here in, which is derived from HSD, reflects information on it. Results show that the index is useful in discriminating melanoma from non-melanoma. Although the present HSI system is different from the previous system [21], the both systems have almost the same performance of melanoma discrimination. This suggests that HSD correctly carry information at a molecular pigmentary level behind the morphology of PSLs independent of HSI types.

To the best of a knowledge, Wallence et.al. [23] used cutaneous spectra in differentiating melanoma from non-melanoma. They also used a fiber to measure a spectrum. Their system measured a spectrum averaged over the view area of fiber every measurement and it was used in analysis. They measured nine to fourteen spectra a patient, i.e., three spectra from the inside of the upper arm, three spectra from the skin surrounding a PSL of suspicious and three to five spectra from the random positions on the PSL. Such a system is hard to say a system suitable for clinical application. The present HSI measures about 27,000 spectra within about 10 seconds. Note that the number of spectra corresponds to that of pixels included in the view area of imaging fiberscope. Thus, more than one measurement is not always needed. Note that the present system has almost the same performance as the system reported by Wallence et.al. Furthermore, we would like to emphasize that the present index has a clear physical meaning.

One SK (No.21) was judged as a melanoma in the present study. Figure 5 (a) and (b) shows its two-dimensional spectral angle color map and false color image, respectively. The spectral angle distribution, i.e., the probability of finding a given spectral angle, for the case No. 21 is shown in Figure 5 (c). The index was calculated with 4.84. The index larger than the threshold value is attributed to the broader spectral angle distribution, see Figure 5 (c). The large spectral angles came from spectra in peripheral regions of the lesion, colored by red in Figure 5(a). These regions rose up and their color suggested that larger amount of melanin was included in comparison with their neighboring regions. Indeed, the intensity of light detected from the regions was too low to obtain reasonable spectra because of much more scattering and absorption, see Figure 5(d) where the dark current level was about 500 counts. A solution to this problem is still under investigation.

The present system is indeed suitable for clinical application. Furthermore, it has also a considerably high level of performance. Although direct comparison of the present with previous systems is difficult, we would like to comment the following. A critical difference between the present and

previous systems is the field of view, which is mainly determined by the magnifying power of objective lens. The higher the magnifying power is, the lower the amount of light detected by a pixel of CCD becomes. In dealing with spectra reflected from PSLs, there may be an optimum magnifying power of objective lens. This is a future problem to us.

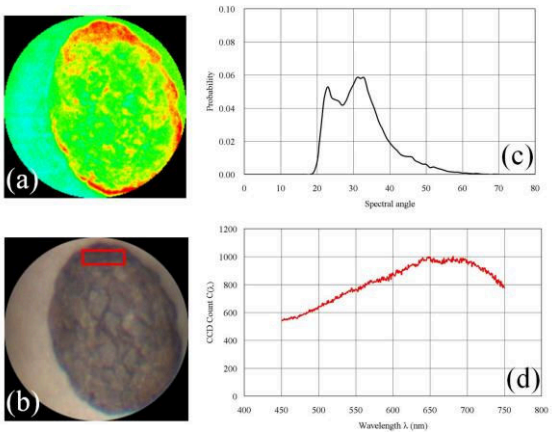

Figure 5. (a) False-color, two-dimensional angle maps for a peripheral part of seborrheic keratosis of case No. 21. (b) The corresponding false color images. (c) Normalized frequency distribution of spectral angle (d)Average CCD count in the red frame of (b). This case is misjudged by the present system. A possible reason why this case is misjudged is.that resonable spectra are not obtained from the periferal regions (red area shown in (a)) because of stronger scattering and absorption.

V. Conclusion

We have developed a HSI attached to imaging fiberscope suitable for clinical application. The melanoma discrimination index has been derived from HSD and it achieved the sensitivity of 100% and the specificity of 94.4% even though the statistical population is still small. It is suggested that the index, which represents variegation at pigmentary molecular level of PSLs through HSD, may get at the essence of melanoma. We are now planning to develop a new device to overcome problems found in studies so far and make a large scale examination in more than one facility.

References

[1] Vital Statistics Japan (Ministry of Health, Labour and Welfare)

[2] T. Matsuda, T. Marugame, K Kamo, K. Katanoda , W Ajiki, T Sobue, and The Japan Cancer Surveillance Research Group, "Cancer incidence and incidence rates in Japan in 2003: based on data from 13 population-based cancer registries in the Monitoring of Cancer Incidence in Japan (MCIJ) project.", Japanese Journal of Clinical Oncology, 39, pp.850-8, 2009

[3] K. Ishihara, T. Saida, F. Otsuka and N. Yamazaki, "Statistical profiles of malignant melanoma and other skin cancers in Japan: 2007 update", International Journal of Clinical Oncology, 13, 1, pp.33-41, 2008

[4] C.A. Morton and R.M. Mackie, "Clinical accuracy of the diagnosis of cutaneous malignant melanoma", Br. J. Dermatol., 138, pp. 283–7, 1998

[5] R.J. Friedman, D.S. Rigel, and A. W. Kopf, "Early detection of malignant melanoma", CA Cancer J Clin. 35, pp.130-151, 1985

[6] H.P. Soyer, J. Smolle, H. Kerl and H Stettner, "Early diagnosis of malignant melanoma by surface microscopy", Lancet, 2, 8562, pp. 803, 1987

[7] F. Nachbar, W. Stolz, T. Merkle, et.al., "The ABCD rule of dermatoscopy", Journal of the American Academy of Dermatology, 30, 4, pp. 551-559, 1994

[8] G. Argenziano, H.P. Soyer, S. Chimenti, et.al., "Dermoscopy of pigmented skin lesions: Results of a consensus meeting via the Internet.", Journal of Academy of Dermatology, 48, 5, pp.679-693, 2003

[9] F. Ercal, A. Chawla, W.V. Stoecker, H.C. Lee and R.H. Moss, "Neural network diagnosis of malignant melanoma from colour images", IEEE Trans. Biomed. Eng., 41, pp. 837–45, 1994

[10] H. Pehamberger, M. Binder, A. Steiner and K. Wolff, "In vivo epiluminescence microscopy: improvement of early diagnosis of melanoma", J. Invest. Dermatol., 100 (suppl), pp. 356S–362S, 1993

[11] H. Kittler, H. Pehamberger, K. Wolff and M. Binder, "Diagnostic accuracy of dermoscopy", Lancet Oncol., 3, pp. 159–65, 2002

[12] M.E. Vestergaard, P. Macaskill, P.E. Holt, and S.W. Menzies,"Dermoscopy compared with naked eye examination for the diagnosis of primary melanoma: a meta-anaysis of studies performed in a clinical setting", Br. J. Dermot. 159, pp.669-676,2008.

[13] J. Neila and H.P. Soyer, "Key points on dermoscopy for siagnosis of melanomas, including difficult to diagnose melanomas, on the trunk and extrenmities", J. Dermat. 38, pp3-9, 2011.

[14] H. Iyatomi, H. Oka, M.E. Celebi, et.al, "An Improved Internet-based Melanoma Screening System with Dermatologist-like Tumor Area Extraction Algorithm", Computerized Medical Imaging and Graphics, 32, 7, pp. 566-579, 2008.

[15] M. Carrara, A. Bono, C. Bartoli, et.al, "Multispectral imaging and artificial neural network:mimicking the management decision of the clinician facing pigmented skin lesions", Phys. Med. Biol., 52, pp. 2599–2613, 2007

[16] http://www.molemate.com/apac/our-product/about-molemate/

[17] S.W. Menzies, L. Bischof, H. Talbot, et.al., "The Performance of SolarScan -An Automated Dermoscopy Image Analysis Instrument for the Diagnosis of Primary Melanoma-", Arch Dermatol., 141, pp. 1388-1396, 2005

[18] M. Elbaum , A.W. Kopf, H.S. Rabinovitz, et.al., "Automatic differentiation of melanoma from melanocytic nevi with multispectral digital dermoscopy: a feasibility study.", J Am Acad Dermatol., 44, 2, pp. 207-18, 2001

[19] T. Vo-Dinh, D.L. Stokes, M.B. Wabuyele, M.E. Martin, J.M. Song, R. Jagannathan, E. Michaud, R.J. Lee and X. Pan, "A hyperspectral imaging system for in vivo optical diagnostics", IEEE Eng.in Med. Biol. Mag., 23, pp. 14855, 2004

[20] B. Khoobehi, J.M. Beach and H. Kawano, "Hyperspectral imaging for measurement of oxygen saturation in optic nerve head", Inv. Ophthal. Vis. Sci., 45, pp. 1464-72, 2004

[21] T. Nagaoka, A. Nakamura, H. Okutani, Y. Kiyohara and T. Sota, "A possible melanoma discrimination index based on hyperspectral data: a pilot study", Skin Research and Technology, doi: 10.1111/j.1600-0846.2011.00571.x, 2011

[22] R. Marchesini, M. Brambilla, C. Clemente, et.al., "In vivo spectrophotometric evaluation of neoplastic and non-neoplastic skin pigmented lesions - 1. Reflectance measurements", Photochem. Photobiol., 53, pp. 77-84, 1991

[23] V.P. Wallace, D.C. Crawford, P.S. Mortimer, R.J. Ott and J.C. Bamber, "Spectrophotometric assessment of pigmented skin lesions: methods and feature selection for evaluation of diagnostic performance", Phys. Med. Biol., 45, pp. 735-751, 2000

[24] M. Osawa and S. Niwa, "A portable diffuse reflectance spectrophotometer for rapid and automatic measurement of tissue", Meas. Sci. Technol., 4, pp. 668-76, 1993

[25] F.A. Kruse, A.B. Lefkoff, J.W. Boardman, et.al, "The spectral image processing system (SIPS)-interactive visualization and analysis of imaging spectrometer data", Remote Sensing of Environment, 44, 2-3, pp. 145-163, 1993

[26] J.A. Swets, "Measuring the accuracy of diagnostic systems", Science, 240, pp. 1285-93, 1988

[27] F. Nachbar,W. Stolz, T. Merkle, et.al., "The ABCD rule of dermatoscopy. High prospective value in the diagnosis of doubtful melanocytic skin lesions", J Am Acad Dermatol., 30, 4, pp. 551-9, 1994